Molecular Therapy
Methods & Clinical Development
Original Article

CRISPR-Cas9-mediated somatic correction of a one-base deletion in the Ugt1a gene ameliorates hyperbilirubinemia in Crigler-Najjar syndrome mice

Giulia Bortolussi,[1] Alessandra Iaconcig,[1] Giulia Canarutto,[1] Fabiola Porro,[1] Filippo Ferrucci,[1] Claudia Galletta,[1] Cristian Díaz-Muñoz,[1] Vipin Rawat,[1] Alessia De Caneva,[1] Olayemi Joseph Olajide,[1] Lorena Zentilin,[1] Silvano Piazza,[1] Luka Bočkor,[1] and Andrés Fernando Muro[1]

[1]International Centre for Genetic Engineering and Biotechnology, Trieste, Italy

(AAV)-mediated episomal gene replacement therapy for monogenic liver disorders is currently limited in pediatric settings due to the loss of vector DNA, associated with hepatocyte duplication during liver growth. Genome editing is a promising strategy leading to a permanent and specific genome modification that is transmitted to daughter cells upon proliferation. Using genome targeting, we previously rescued neonatal lethality in mice with Crigler-Najjar syndrome. This rare monogenic disease is characterized by severe neonatal unconjugated hyperbilirubinemia, neurological damage, and death. Here, using the CRISPR-*Staphylococcus aureus* Cas9 (*Sa*Cas9) platform, we edited the disease-causing mutation present in the Ugt1a locus of these mice. Newborn mice were treated with two AAV8 vectors: one expressing the *Sa*Cas9 and single guide RNA, and the other carrying the *Ugt1a* homology regions with the corrected sequence, while maintained in a temporary phototherapy setting rescuing mortality. We observed a 50% plasma bilirubin reduction that remained stable for up to 6 months. We then tested different Cas9:donor vector ratios, with a 1:5 ratio showing the greatest efficacy in lowering plasma bilirubin, with partial lethality rescue when more severe, lethal conditions were applied. In conclusion, we reduced plasma bilirubin to safe levels and partially rescued neonatal lethality by correcting the mutant *Ugt1a1* gene of a Crigler-Najjar mouse model.

INTRODUCTION

The Crigler-Najjar syndrome is an ultra-rare recessive pediatric disorder (affecting <1 newborn per million live births) caused by mutations in the uridine diphosphate glucuronosyltransferase1A1 (*UGT1A1*) gene, which is responsible for the production of the liver-specific UGT1A1 enzyme.[1–3] The absence or reduced activity of UGT1A1 results in severe unconjugated hyperbilirubinemia from birth, with a lifelong risk of permanent neurological damage, kernicterus, and death.[1,4,5] Patients are treated from birth with intensive phototherapy (12–14 h/day) to reduce the levels of neurotoxic unconjugated bilirubin in blood and tissues.[6] However, this approach becomes less effective with age. To date, no curative therapy is available, with the exception of liver transplantation, an option with many limitations and risks,[7,8] emphasizing the need for novel curative therapies to be developed.

Recent clinical trials have demonstrated the potential of gene replacement therapy to cure monogenic liver diseases in adults.[9–13] However, major concerns still remain, such as the duration of transgene expression, the risk of adeno-associated virus (AAV)-mediated tumorigenesis caused by random insertion of the promoter-containing construct,[14,15] and the potential loss of viral episomal DNA in duplicating hepatocytes during liver growth in neonatal and pediatric settings and in pathological liver conditions.[16–18]

Gene editing and genome targeting strategies have shown promising potential to permanently correct the diseased genome.[19,20] The required rate of correction varies depending on both the disease type and the presence or absence of growth advantage of the corrected cells. In fact, in spite of low initial editing/targeting rate, the expansion of corrected hepatocytes due to a growth advantage resulted in therapeutic correction levels in studies performed in mouse models of fumarylacetoacetate hydrolase (FAH) and methylmalonic acidemia diseases.[21–24] In the case of hemophilia B, a disease in which corrected cells have no proliferative advantage, only 2%–3% of wild-type (WT) coagulation factor IX activity is sufficient to revert the bleeding phenotype from severe to moderate[25] and, thus, lower levels of correction are required. Therapeutic correction was obtained by gene editing of the disease-causing mutation using the CRISPR-Cas9 platform and by gene targeting with or without the use of nucleases, both in neonates and adult animals.[26–32]

In the case of the Crigler-Najjar syndrome, neonatal treatment with gene replacement therapy results in the partial loss of the episomal vector, associated with hepatocyte duplication during liver growth.[16] In contrast, long-term therapeutic efficacy is observed after

Received 10 February 2023; accepted 16 November 2023;
https://doi.org/10.1016/j.omtm.2023.101161.

Correspondence: Andrés Fernando Muro, International Centre for Genetic Engineering and Biotechnology (ICGEB), Padriciano 99, Trieste, TS 34149, Italy.
E-mail: andres.muro@icgeb.org

This is an open access article under the CC BY-NC-ND license (http://creativecommons.org/licenses/by-nc-nd/4.0/).

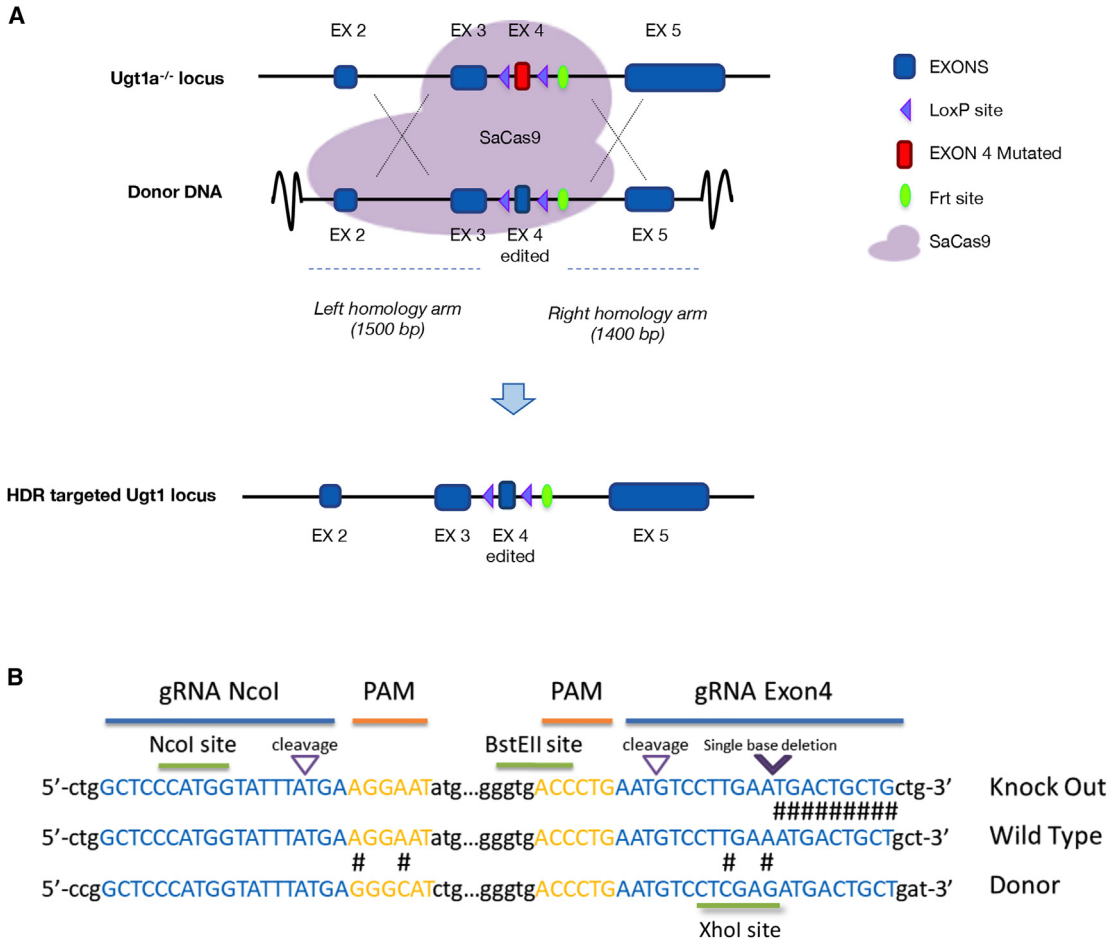

Figure 1. General strategy of AAV8-mediated gene editing in the *Ugt1a* gene in combination with the CRISPR-*Sa*Cas9 platform

(A) Schematic representation of the experimental strategy. Recombination of the donor vector (donor DNA; containing the corrected exon 4 and flanked by *Ugt1a* homology regions results in the HDR-targeted correction of the *Ugt1a* locus. Rectangles represent exons; thin black lines, introns; AAV-inverted terminal repeats (ITR), wavy lines. (B) The mutated (knockout), WT, and donor sequences are shown. The sgRNAs and protospacer adjacent motif (PAM) sites (gRNA NcoI and gRNA Exon 4), the *Sa*Cas9 cleavage sites, and the enzyme restriction sites (NcoI, BstEII, and XhoI) are indicated. Mismatches between the sequences are indicated by pound signs.

site-specific integration of a promoterless *Ugt1a1* cDNA into the albumin locus, rescuing neonatal lethality of mice with Crigler-Najjar syndrome.[33,34] While the approach without the use of engineered nucleases reduced plasma bilirubin to safe levels,[34] the use of the *Staphylococcus aureus* Cas9 (*Sa*Cas9) platform improved efficacy resulting in complete correction, with total plasma bilirubin values similar to the WT and supraphysiological levels of the Ugt1a1 enzyme.[33] Herein, we explored the therapeutic potential of the CRISPR-SaCas9 platform in restoring normal bilirubin levels and rescuing newborn lethality in a Crigler-Najjar mouse model by correcting a one-base deletion in the *Ugt1a* gene.

RESULTS

In vitro selection of single guide RNAs

To determine if correcting the one-base deletion present in the *Ugt1a* locus of a mouse model of the Crigler-Najjar syndrome[35,36] could restore normal bilirubin levels in these hyperbilirubinemic animals, we designed a strategy based on CRISPR-Cas9-mediated homology-directed repair (HDR) by using a donor construct containing a corrected version of the exon 4 flanked by homology arms of 1.6 kb (Figure 1A). To facilitate the identification of the edited alleles, an XhoI restriction enzyme site was inserted at the place of the one-base correction by changing the codon sequences without modifying the primary sequence of the protein (Figure 1A).

First, we created a set of single guide RNAs (sgRNAs) both for *Streptococcus pyogenes* Cas9 (*Sp*Cas9) and *Sa*Cas9, targeting sequences near the position of the mutation (Figure S1). These sgRNAs were then tested *in vitro* by transient transfection of a plasmid expressing the Cas9 (*Sp*Cas9 or *Sa*Cas9) and the sgRNA, and an HDR reporter plasmid containing the mutated or WT *Ugt1a* exon 4 flanked by the dead halves of the luciferase cDNA.[37] Luciferase activity is

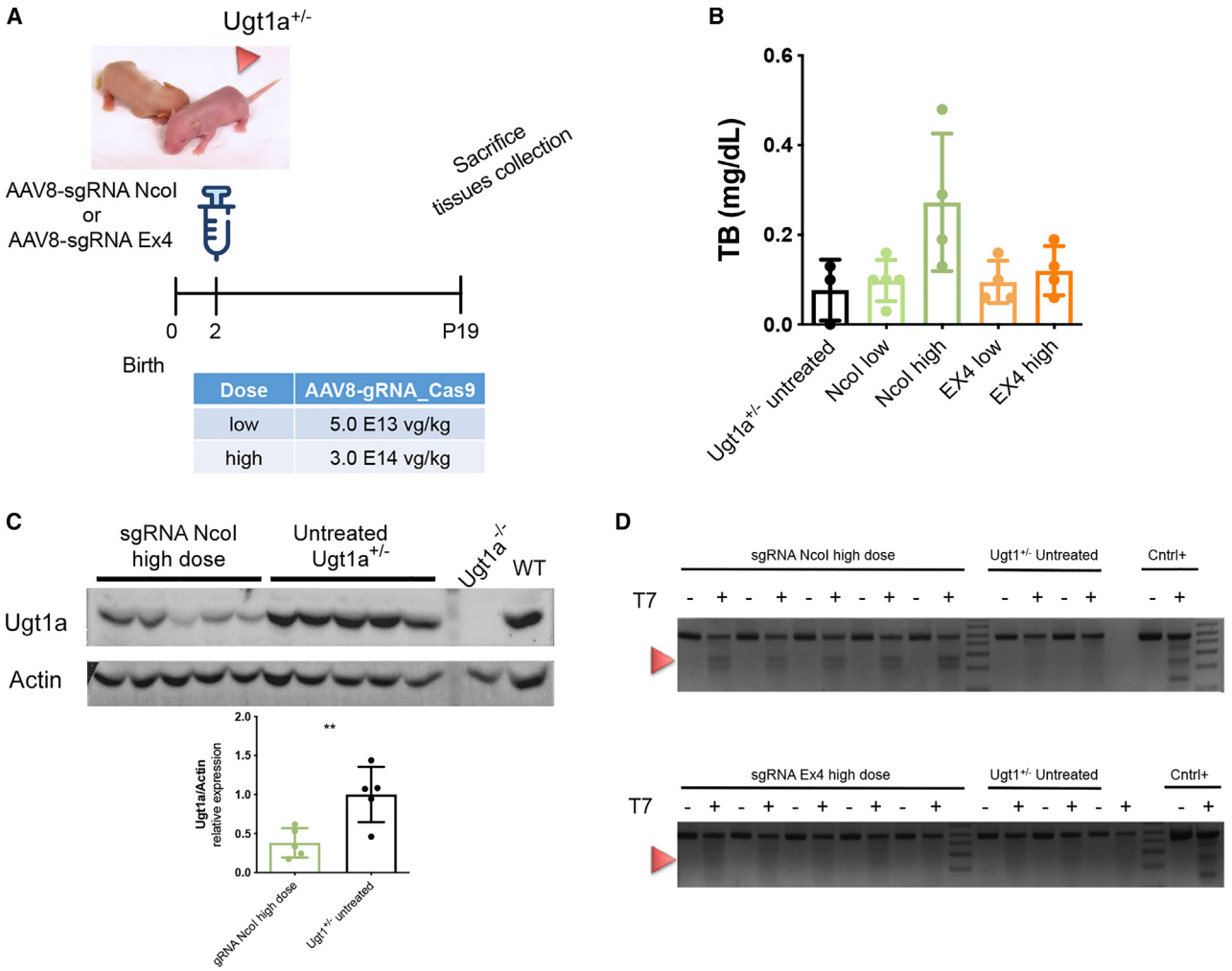

Figure 2. Genome editing of heterozygous mice results in a decrease of Ugt1a enzyme

(A) Scheme of the experimental design. P2 heterozygous mice were transduced with AAV8-expressing the *Sa*Cas9 and the sgRNA NcoI or sgRNA Ex4. Two doses were tested (5.0E13 vg/kg and 2.5E14 vg/kg). Mice were sacrificed at P19 and blood and tissues collected. (B) Plasma bilirubin levels at sacrifice (mean ± SD). (C) Western blot analysis of liver protein extracts. Densitometric quantification of the WB bands (lower panel). Student t test: **, $p < 0.01$. (D) The results for the sgRNA NcoI and sgRNA Ex4 T7E1 assays are shown. "+" and "-" indicate addition or not of the T7 endonuclease. The positive control consisted of an equimolar mixture of amplicons derived from two sequences with several mismatches.

restored upon recombination, enhanced by the double-strand break (DSB), and its activity correlates with Cas9 DSB digestion rate[37] (Figure S2A). We observed that sgRNAs "NcoI" and "Exon4" (both from *Sa*Cas9) were the most active ones (Figures S2B and S2C). The "NcoI" sgRNA target site is located 121 bp upstream of the deletion, immediately downstream of a NcoI restriction enzyme site, while the "Exon4" sgRNA target region overlaps with the one-base deletion (Figures 1B and S1). When we tested the "Exon4" sgRNA in a construct containing the WT exon 4 sequence, luciferase activity was at background levels, with a significant increase in luciferase activity when co-transfected with a construct containing the mutated exon 4. In contrast, the "NcoI" sgRNA targeted both WT and mutant reporter constructs with similar efficacy (Figure S2D).

In vivo SaCas9 activity in Ugt1a$^{+/-}$ mice

To test the activity of the *Sa*Cas9 and sgRNA *in vivo*, heterozygous FVB/NJ Ugt1a$^{+/-}$ mice were used. We performed an intravenous injection in postnatal day 2 (P2) mice with the AAV8 vector coding for *Sa*Cas9 and the sgRNA-NcoI or sgRNA-Exon 4 sgRNAs. For each treatment we tested two doses by each of the AAV8 vectors (5.0E13 vg/kg and 3.0E14 vg/kg, for low and high doses, corresponding with 1.0E11 vg/pup and 5.0E11 vg/pup respectively) (Figure 2A). Mice were sacrificed at P19 and blood and tissues were collected for analysis. Quantification of plasma bilirubin showed an increase in the levels in the group treated with the high dose of AAV-NcoI, although the difference was not statistically significant (Figure 2B), suggesting efficient targeting and inactivation through the

non-homologous end joining (NHEJ) repair mechanism of the WT *Ugt1a* allele in a large proportion of liver cells. This result was supported by the western blot analysis of liver protein samples of those animals, which showed a significant decrease in Ugt1a protein levels (Figure 2C). T7 nuclease analysis of liver DNA samples also showed greater efficiency of the NcoI sgRNA, compared with the Exon 4 sgRNA (Figure 2D), in line with the results of plasma bilirubin and Ugt1a protein levels in the high-dose sgRNA-NcoI treated mice (Figures 2B and 2C).

Biodistribution analysis of viral DNA and *Sa*Cas9 mRNA levels showed that the liver was the main target organ that was targeted (Figures S3A–S3D). The groups that were given the higher AAV dose presenting higher viral genome copies (vgcs) and mRNA expression than the groups that were given the lower AAV dose (Figures S3B and S3C). Unexpectedly, we observed expression of *Sa*Cas9 also in the heart, suggesting that the thyroxine-binding globulin promoter has low tissue specificity (Figures S3C and S3D).

In vivo gene editing in Ugt1a$^{-/-}$ mice

To determine the real efficacy of the approach to correct the phenotype, Ugt1a$^{-/-}$ mice were treated with two AAV viruses at P3. One virus had the corrected version of *Ugt1a* exon 4 flanked by homology arms (AAV8-Ugt-Donor), and the other one coded for the *Sa*Cas9 nuclease and the sgRNA-NcoI or sgRNA-Exon4 (AAV8-sgRNA-NcoI and AAV8-sgRNA-Exon4, respectively). Since all untreated Ugt1a$^{-/-}$ mice die within 2 weeks after birth, to solely evaluate the potential of the procedure to decrease plasma bilirubin, mice were kept under phototherapy (PT) for 15 days (P0–P15 PT), a condition that fully rescues mortality,[36] and were sacrificed at P30 (Figure 3A). It is important to note that the beneficial effect of the PT treatment on bilirubin plasma levels vanishes 2–3 days after its discontinuation. Analysis of plasma bilirubin at P30 showed a statistically significant decrease in the group treated with the sgRNA-NcoI (a 42% decrease compared with the untreated group), while the animals treated with the sgRNA Exon4 showed a minor decrease (9.5% reduction) (Figure 3B). Determination of vgcs showed no difference between the groups, indicating that transduction efficiency was similar in both groups (Figure 3C).

To have a deeper insight into the editing rate of the *Ugt1a* locus, we analyzed the PCR product derived from liver genomic DNA of the targeted region using primers that detect only the endogenous allele. We digested the PCR product with NcoI and XhoI restriction enzymes, to determine the molecular events at the target site, i.e., the inactivation of the NcoI site and the incorporation of a new XhoI in the sequence. The NcoI site is located 3 bases upstream of the cleavage site of the *Sa*Cas9-sgRNA NcoI and its inactivation will indicate NHEJ correction, while the XhoI is absent in the natural allele, but it will be inserted upon successful HDR-mediated editing of the endogenous exon 4 (Figure 3D). Thus, the presence of an undigested higher molecular weight band could result from the imprecise NHEJ-mediated repair of the *Sa*Cas9-induced DSB (indicated with red asterisks in lanes 5 and 6). In contrast, the presence of an extra band of 340 bp after the digestion with XhoI indicates precise donor-mediated homologous recombination in exon 4 of the Ugt1a locus. We observed a high proportion of NcoI-undigested band, while the levels of the new band generated after XhoI digestion were much lower (Figure 3D, red asterisks in lanes 13–16). This suggests that most of the DSBs generated by the NcoI sgRNA were repaired by the NHEJ repair mechanism, and not by HDR. In addition, rough quantification of the XhoI band intensity by ImageJ indicated that the HDR in liver was higher in mice treated with the NcoI sgRNA than in the Ex4 sgRNA-treated animals (2.3% vs. 1.3%, respectively), in line with the plasma bilirubin results.

A long-term experiment with the sgRNA NcoI (AAV-Cas9 to AAV donor ratio of 1:1) showed stable levels of plasma bilirubin in treated animals. This suggests that the modification of the *Ugt1a* gene was transmitted to daughter hepatocytes after cell duplication during liver growth (Figure 3E).

In vivo gene editing partially rescues Ugt1a$^{-/-}$ mice mortality

Aiming at improving gene editing efficacy, we tested two additional donor-to-*Sa*Cas9 AAV vector ratios. Ugt1a$^{-/-}$ newborn animals were treated at P3 with the two AAV vectors, with AAV-Cas9 to AAV donor ratios of 1:2 and 1:5, and blood was collected at P30 (Figure S4A). We observed an inverse correlation between plasma bilirubin levels and AAV donor dose, also comparing with the 1:1 ratio used in Figure 3D. In fact, the mean plasma bilirubin was 4.1 mg/dL in the group treated with a 1:5 ratio (Figure S4B).

These mice were followed to assess long-term effects and were sacrificed after 6 months (Figure 4A). Plasma bilirubin levels remained constant in all groups of mice, with animals receiving the 1:5 AAV vector ratio presenting lower bilirubin levels (Figure 4B). Upon sacrifice at 6 months after injection, we performed a PCR of the genomic region and subsequent analysis by restriction enzyme digestion of DNA isolated from the liver. Digestion of the PCR product with NcoI presented a prominent higher molecular weight band corresponding with the absence of the NcoI site. No major differences were observed among the different treatment donor-to-*Sa*Cas9 ratios (Figures S5A and S5B). In contrast, the intensity of the band generated after XhoI digestion increased with the donor AAV dose, inversely correlating with the levels of plasma bilirubin (1.4%, 1.8%, and 2.2% for 1:1, 1:2, and 1:5 ratio, respectively) (Figure S5C). Quantification of vgcs showed a dose-response effect for the donor construct, while the levels of the gRNA_*Sa*Cas9 vector were similar in the three groups (Figure S6). We then performed an RT-PCR from the RNA of treated animals and cloned the resulting product. Sequencing showed the presence of edited clones, without the deletion and containing a new XhoI site in the edited region, as well as the NcoI site, with a series of base modifications in this region, that were included to eliminate a potential cryptic splice site (Figures 4C and S5D), confirming the success of the editing procedure. These results were further confirmed by performing a next-generation sequencing (NGS) analysis of the edited region, showing between 0.81% and 1.44% of editing rate (Figure S7 and Table S1). The NGS analysis also showed that the cleavage site contained 15%–20% of

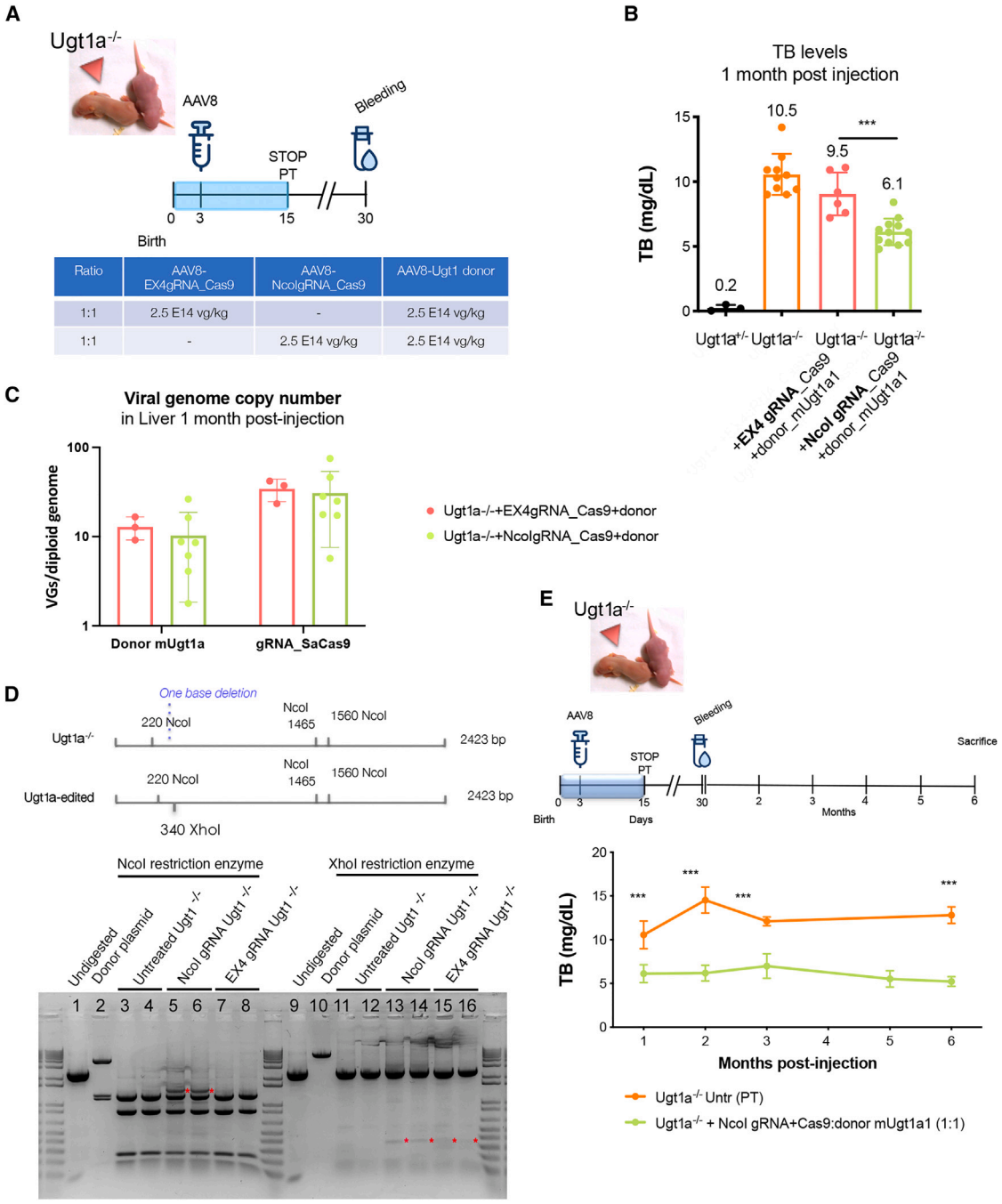

Ratio	AAV8-EX4gRNA_Cas9	AAV8-NcoIgRNA_Cas9	AAV8-Ugt1 donor
1:1	2.5 E14 vg/kg	-	2.5 E14 vg/kg
1:1	-	2.5 E14 vg/kg	2.5 E14 vg/kg

Figure 3. Treatment of homozygous mutant mice results in a significant decrease in plasma bilirubin levels

(A) Short-term experiment. Scheme of the experimental design. P3 homozygous mutant mice were transduced with two AAV8 vectors: one containing the corrected exon 4 plus homology arms (AAV8-Ugt1a-donor), plus another one expressing the *Sa*Cas9 and the sgRNA NcoI or sgRNA Ex4. A single dose/vector ratio was tested (2.5E14 vg/kg of each vector). PT treatment (since birth) was stopped at P15. Mice were sacrificed at P30 and blood and tissues collected. (B) Plasma bilirubin levels at sacrifice (at each time point the mean ± SD are indicated). One-way ANOVA, ***$p < 0.001$. (C) Determination of vgcs (mean ± SD). (D) PCR of liver genomic DNA followed by restriction digestion analysis. The PCR reaction is designed to only amplify genomic DNA, and not the donor DNA. The position of the restriction sites are indicated in the schemes. The asterisks indicate the bands originated after NHEJ (NcoI restriction, lanes 5 and 6) or HDR (XhoI restriction, lanes 13–16). (E) Long-term experiment. Mice were transduced as described in (A). Only the AA8-NcoI-SgRNA-*Sa*Cas9 vector was tested. Blood samples were taken at different time points. Mice were sacrificed at 6 months post injection. Plasma bilirubin levels are shown in the graph. Mixed-effects analysis: time, $p < 0.01$; Treatment, $p < 0.0001$; time x treatment, $p < 0.001$; Sidak's multiple comparison tests: $p < 0.001$ for all timepoints.

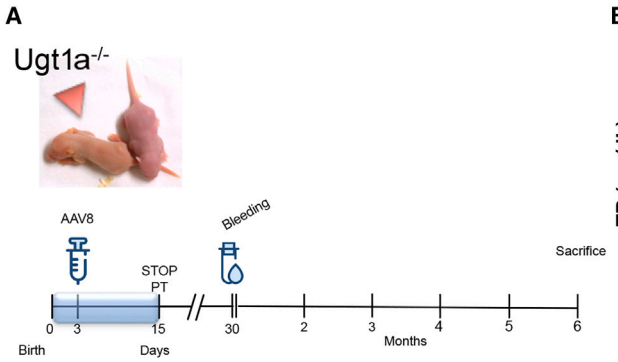

Ratio	AAV8-NcoIgRNA_SaCas9	AAV8-Ugt1 donor
1:1	2.5 E14 vg/kg	2.5 E14 vg/kg
1:2	2.5 E14 vg/kg	5.0 E14 vg/kg
1:5	2.5 E14 vg/kg	1.2 E15 vg/kg

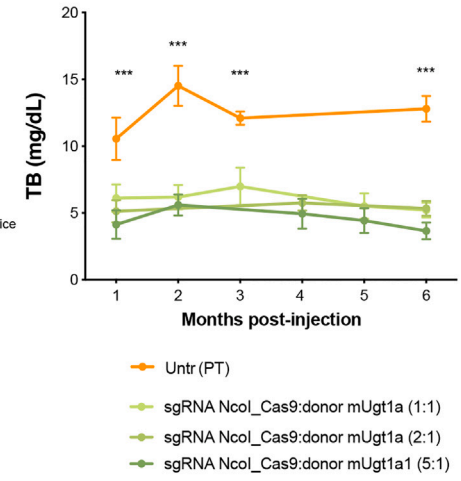

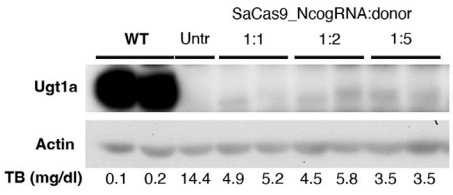

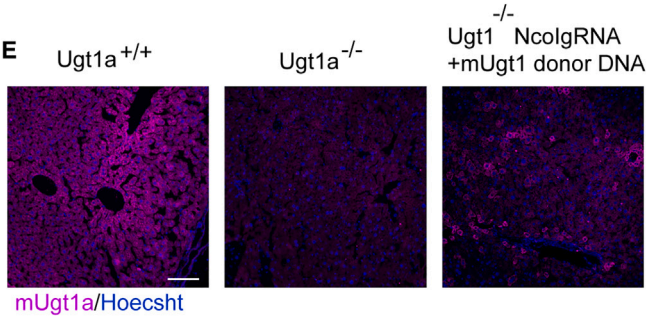

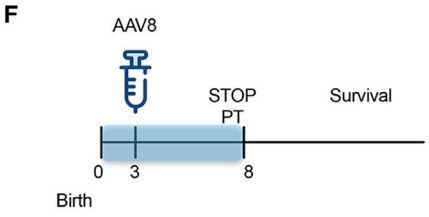

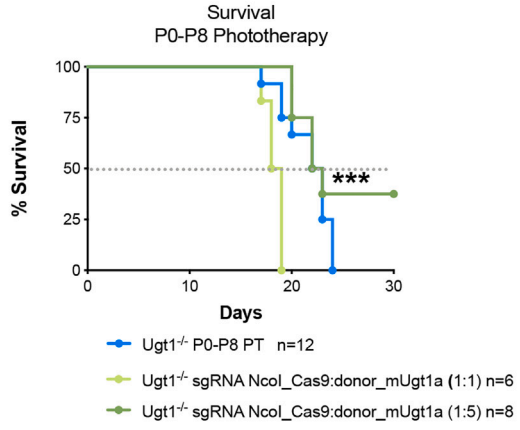

(legend on next page)

insertions/deletions (INDELS) (Figure S7), confirming the results observed after NcoI enzyme restriction digestion and indicating that the *Sa*Cas9 efficiently digested the target site, which was mainly corrected by the NHEJ DNA repair mechanism. Unexpectedly, these events occurred a few bases upstream of the theoretical *Sa*Cas9 cleavage site. Increasing the amount of the donor DNA resulted in increased editing efficiency. Western blot analysis of liver protein extracts confirmed the results of Figures 4B and 4C, with the presence of a stronger Ugt1a signal in the groups treated with the higher donor-to-*Sa*Cas9 ratios (Figure 4D). Immunofluorescence staining of liver samples showed the presence of clusters of Ugt1a-positive cells, suggesting that the correction was transmitted to daughter cells (Figure 4E). Hematoxylin and eosin and trichrome staining showed normal histological features in liver sections of treated animals (Figure S8).

Finally, to determine the efficacy of the procedure in more severe, lethal, hyperbilirubinemic conditions, we applied PT up to P8 (P0–P8 PT) (Figure 4F), a treatment that results in the death of all animals before P21,[36] but a time window that allows gene editing and expression of the corrected transgene. We observed that all animals that were PT treated or PT treated with the 1:1 ratio died, while 40% of the mice who were treated with the PT and 1:5 AAV vector ratio survived, having plasma bilirubin levels of 3.3 mg/dL at M6 (Figure 4F).

To gain insight into the safety of the procedure, we assessed the risks of nuclease off-target activity. We performed an *in silico* prediction analysis of potential off-target sites with bioinformatics software. We found no off-target sites having fewer than three nucleotide mismatches. Since we previously found that *Sa*Cas9 INDELs were not present in off target sites containing four mismatches,[33] we further investigated predicted off-target sites that contained three or fewer mismatches. Only four were detected: three of them were in the introns of *Rtkn2*, *Wwox*, and *Nmnat3* genes, while the last one was in an intragenic region of chromosome 7 (*chr7-Olrf545*). These regions were PCR amplified and subjected to deep sequence analysis. We did not observe the presence of INDELs or single nucleotide polymorphisms in the samples from either treated or untreated animals above background levels, providing experimental support for the safety of the approach.

DISCUSSION

The present work explores the use of the CRISPR-Cas9 technology to correct a somatic single-base mutation present in the endogenous *Ugt1a* locus of a Crigler-Najjar mouse model. The mutant allele contains a one-base deletion in the exon 4 of the *Ugt1a* gene, generating a null mutation.[35] Our results suggest that correction of 2%–3% of the endogenous *Ugt1a* alleles in hepatocytes is sufficient to ameliorate hyperbilirubinemia in mice with Crigler-Najjar syndrome, partially rescuing neonatal mortality. These results are in line with previous data in which transduction with an episomal rAAV vector expressing the *hUGT1A1* cDNA under the control of the α1-antitrypsin promoter resulted in 5%–8% of Ugt1a1 liver activity, with a significant decrease in plasma bilirubin levels and fully rescuing mortality.[16] Similarly, hepatocyte transplantation in patients with Crigler-Najjar syndrome showed that 5% of transplanted hepatocytes resulted in an improvement in plasma bilirubin levels.[38] Previous studies using a promoterless gene targeting strategy into the albumin gene without the use of nucleases showed that 5%–6% of WT protein levels, resulting from a recombination rate of approximately 0.03%,[34] was sufficient to completely rescue from neonatal mortality. A similar approach, but with the use of *Sa*Cas9, resulted in supraphysiological levels of Ugt1a1, with a recombination rate of 3.6%.[33] However, the latter approaches relied on the insertion of a correct copy of the *Ugt1a1* cDNA into the albumin locus, ensuring exceptionally high transcription rates of the transgene.[27] Here, instead, we ameliorated hyperbilirubinemia by editing the disease-causing mutation, and the corrected allele remained under the control of the endogenous *Ugt1a* gene promoter. Important differences between these approaches are present, both in the strategy and in the results, associated with the robust transcription of the targeted gene by the endogenous albumin promoter. In fact, even if the correction rate obtained here was superior to that of the GeneRide approach without nucleases, the rescue from neonatal mortality was only partial, with a correction of between 0.9% and 1.44% of the mutated alleles. These differences are probably related to the different transcription levels observed for the albumin and *Ugt1a1* genes (Figure S8), suggesting that editing rates at the *Ugt1a* locus should be further improved to reach complete protection from hyperbilirubinemia. However, the editing rates observed here were in line with the biological results (partial reduction of plasma bilirubin and partial rescue from mortality) and these numbers are probably underestimated because the editing event occurred in one allele per hepatocyte, and we analyzed the whole liver, which also contains a significant proportion of non-parenchymal cells. Identification of more efficacious sgRNAs, optimization of the length of the homology arms in the donor construct, and simultaneous temporary treatment with NHEJ inhibitors or HDR enhancers

Figure 4. Genome editing of homozygous mutant mice partially rescues neonatal mortality

(A) Scheme of the experimental design. Neonatal mutant mice were treated with AAV8-NcoI sgRNA-Cas9 and AAV8-Ugt1a-donor vectors, at different ratios. PT treatment (since birth) was stopped at P15. Blood samples were taken at different time points. Mice were sacrificed at 6 months post injection. (B) Plasma bilirubin levels (the 1:1 vector ratio shown in Figure 3E was included for comparison; at each time point the mean ± SD are indicated). Mixed-effects analysis: time, $p < 0.01$; Treatment, $p < 0.0001$; time x treatment, $p < 0.001$; Sidak's multiple comparison tests: $p < 0.001$ for all timepoints. (C) Liver *Ugt1a* mRNA was RT-PCR amplified, cloned, and sequenced. The WT (mUgt1a WT), mutant (Ugt1a$^{-/-}$), and edited cDNA are shown. Restriction sites and differences are indicated. (D) Western blot analysis of liver protein extracts. Actin was used as internal control. The plasma bilirubin levels (mg/dL) are indicated below each lane. (E) Immunofluorescence staining of liver samples in Ugt1a$^{+/+}$-, Ugt1a$^{-/-}$-, and Ugt1a$^{-/-}$-edited mice. Sections were stained with anti-Ugt1a antibody (pink) and nuclei were counterstained with Hoechst (blue). Images were acquired with 20× magnification objective. The white bar corresponds with 100 μm. (F) Mutant mice were treated with AAV8-NcoI sgRNA-Cas9 and AAV8-Ugt1a donor vectors, at different ratios, with the same doses used in (A). PT treatment (since birth) was stopped at P8, a condition that results in death of all untreated animals. Kaplan-Meier survival curve of untreated and treated groups. Log rank (Mantel-Cox) test. ***$p < 0.001$.

at the moment of AAV vector administration may be necessary to reach more efficacious gene editing rates and increased therapeutic levels.[39,40]

While these differences may pose a limit to the overall efficacy of the method, the presence of a corrected *Ugt1a* allele ensures its natural expression control, producing physiological levels of the corrected protein in hepatocytes in all situations, although the potential transfer of this approach to the clinic may be limited by the need to perform mutation-specific strategies. Other approaches such as the overexpression of a therapeutic transgene by a robust liver-specific promoter or in the permanent insertion of the corrected cDNA into a safe harbor locus may result in the production of supra-physiological levels of the transgenic protein, raising safety concerns. While endoplasmic reticulum stress was observed with overexpression of the coagulation factor VIII in mice,[41] no liver damage was observed even 10 months after the therapeutic *UGT1a1* transgene was inserted into the albumin locus, notwithstanding that targeted hepatocytes expressed about 60 times the normal Ugt1a1 levels.[33] We observed normal histology in liver samples of treated animals, and we observed no off-target activity of the nuclease at the predicted sites that were examined, supporting the safety of the procedure. However, other concerns exist, such as immunogenicity of the nuclease, and potential long-term effects cannot be excluded when transferred to the clinic. This should be very carefully examined.

Other approaches reached a higher proportion of edited cells associated to the growth advantage of the corrected cells.[22,42] In the case of FAH, the proportion of corrected hepatocytes with initial expression of the WT FAH protein was in the range of approximately 1 in 250 liver cells. They expanded 1 month after injection 33.5% of the total hepatocytes.[22] In contrast, corrected cells in Crigler-Najjar mice or patients do not present any selective advantage compared with mutant hepatocytes. This fact poses important restrictions on the approach, as the therapeutic efficacy depends only on the original gene correction rate. In other cases, in which no growth advantage was present, the required rate of recombination varies among the different diseases. For example a rate of HDR correction of 0.7% in the *G6PC* gene was sufficient to correct the metabolic abnormalities present in a mouse model of glycogen storage disease type Ia.[43] In the case of ornithine transcarbamylase deficiency (Spf^{Ash} mouse model), amelioration of the phenotype was obtained with higher correction rates than the ones observed here, which were in the range of 10% of corrected hepatocytes.[44] While the AAV doses we used here were similar to those used by Yang et al.,[44] the differences may be associated with the *in vivo* targeting efficacy of the sgRNA. Another possibility could be that Cas9 activity may be influenced by locus-specific features independent of the target sequence, modulating the accessibility and chromatin state of the different loci,[45] a hypothesis that needs further study.

Here, we took advantage of the high proliferative condition of newborn mice, a condition in which HDR-mediated DSB repair is highly active.[46] In the case of potential treatments of more mature livers with reduced mitotic activity, other strategies may be implemented, such as the use of compounds enhancing AAV-homologous recombination.[39]

In summary, this study provide evidence for the first time that Cas9-mediated genetic correction in the endogenous Ugt1a locus in a mouse model of the Crigler-Najjar syndrome type I ameliorates hyperbilirubinemia. The strategy proposed here confirms the potential use of the CRISPR-Cas9 platform as a versatile tool in precision medicine. However, the clinical translation of the approach still needs important improvements and further experimentation to completely rule out all safety concerns.

MATERIALS AND METHODS

Animals

Animals were housed and handled according to institutional guidelines, and experimental procedures approved by International Center for Genetic Engineering and Biotechnology (ICGEB) review board, with full respect to the EU Directive 2010/63/EU for animal experimentation, and by the Italian Health Minister (authorization N. 996/2017-PR). All animal experiments conform to all relevant regulatory standards. $Ugt1a^{-/-}$ mice used had at least a 99.8% FVB/NJ genetic background,[36] obtained after more than 10 backcrosses with FVB/NJ WT mice. Males and females were used indistinctly for the experiments. Mice were maintained in the ICGEB animal house unit in a temperature-controlled environment with 12 h light-dark cycles and received a standard chow diet and water *ad libitum*. AAV-treated mice at different postnatal days (P2 or P3) were retro-orbitally injected with the indicated vectors and dose, as described in the experimental design of the Figures 2A, 3A, and 4A.

Bilirubin determination in plasma

Blood was obtained from anesthetized mice by facial vein bleeding. Bilirubin was determined in plasma as described.[36]

Cell transfection

HeLa cells were transfected using Lipofectamine 2000 reagent (Invitrogen) following the manufacturer's guidelines. Cells were plated in p12 or p24 well plates to be 75%–90% confluent at transfection. Lipofectamine 2000 and DNA were diluted at the desired concentration with Opti-MEM Reduced Serum Medium. The diluted DNA was added to diluted Lipofectamine 2000 Reagent (1:1 ratio). Complete medium was removed, washed with PBS, and replaced with antibiotics-free medium. Cells were analyzed 24 h after transfection.

Construction of sgRNAs-*Sa*Cas9 and donor DNA AAV vectors

The donor vector was designed with the following properties: the full length of the donor recombination region was 3,942 bp consisting of codon optimized exon 4 region of *Ugt1a* of 706 bp flanked by left arm of homology of 1,593 bp and right arm of homology of 1,643 bp in length. Homology region was flanked by NotI restriction sites for subcloning into the donor DNA AAV. The recombination construct also contained *loxP*1, *loxP*2, and Frt sites at the positions corresponding to the mouse genome, as they are present in the genome of our mouse

model.[35] Codon optimization without change in primary protein sequence was performed to introduce an XhoI site and avoid activation of a potential cryptic splice site. After design, the sequence synthesis was performed by GeneScript and obtained sequence cloned into the donor DNA AAV. Accuracy of the final construct was verified by restriction digestion and sequencing of the complete region. The full sequence of all vectors is available in Figures S10–S12.

DNA purification and viral genome particles quantification

DNA extraction was performed with Wizard SV Genomic DNA Purification System (Promega) according to manufacturer's instructions. DNA was purified from liver, heart, and brain tissue collected from mice. For the liver and brain, around 15 mg powder were used while one-half of the heart was used directly, without producing the powder (to maximize the yield). DNA yield was determined by NanoDrop 1000 spectrophotometer (Thermo Fisher Scientific). VGP was determined as previously described[33,39] using the primers listed in Table S2.

Genomic DNA preparation from cells and liver samples

Genomic DNA was prepared from cells as briefly described below. Cells were lysed in 50 mM Tris-HCl pH 7.5, 100 mM EDTA, 0.5% SDS, and 200 μg/mL protease K for 1 h at 37°C and centrifuged for 10 min at maximum speed. Genomic DNA was precipitated with 2-propanol and resuspended in TE buffer after centrifugation and washing.

Whole livers were reduced to powder with a mortar and liquid nitrogen, and stored at −80°C. Genomic DNA was prepared by incubating 25–50 mg liver powder overnight at 56°C in 500 μL lysis buffer (50 mM Tris-HCl pH 8, 100 mM EDTA pH 8, 1% SDS, 100 mM NaCl) containing fresh Proteinase K at a final concentration of 100 μg/mL. The day after, the samples were centrifuged at maximum speed for 10 min at RT. Genomic DNA was precipitated by centrifuging at maximum speed for 10 min with 500 μL 2-propanol. Genomic DNA was resuspended in TE buffer after centrifugation and washing.

Luciferase gene report assay

The assay was performed by using a reporter plasmid containing an inactive luciferase cDNA[37] specifically designed to measure Cas9 activity. The luciferase cDNA contains a 548-bp-repeated region interrupted by the *Ugt1a* exon 4 and flanking introns. If Cas9 generates a DSB in the target sequence it could trigger a recombination event that restores luciferase gene. In detail, pGL3-UGT-ex4(wt), contains firefly luciferase cDNA interrupted by an WT exon 4 sequence; in pGL3-UGT-ex4(mut) firefly luciferase is interrupted by a mutant exon 4 sequence; pGL3 basic vector, contains firefly luciferase cDNA; and phRG-TK-Renilla (Promega), containing Renilla luciferase. HeLa cells were transfected with various combinations of reporter and pX601 plasmids containing sgRNA of interest. The latter expresses the *Sa*Cas9 cDNA and the sgRNA. The sgRNAs within these plasmids were directed against the mutated *Ugt1a* exon4 sequence (pX601-gRNA4(ex4)), the NcoI site present in both WT and mutant exon 4 (pX601-gRNA(Nco)) and against albumin (pX601-gRNA(Alb)). A group of cells was treated with a standard pGl3 vector and was used as transfection positive control. After 24 h, cells were collected and quantitation of luminescent signal from each of the luciferase reporter enzymes was performed immediately using Dual-Luciferase Reporter Assay System (Promega). Luminescence was measured using a single sample luminometer. Signal was expressed as ratio between firefly and Renilla luminescence.

PT treatment

Ugt1a$^{-/-}$ and littermate newborns were exposed to blue fluorescent light (450 nm wavelength, 20 μW/cm^2/nm, Philips TL 20W/52 lamps) for 12 h/day (synchronized with the light period of the light/dark cycle) up to P8 or P15 as indicated, and then maintained under normal light conditions. The intensity of the emitted light was monitored monthly with an Olympic Mark II Bili-Meter (Olympic Medical).[35]

Ugt1a$^{-/-}$ control mice were obtained by treating mutant mice with PT for 15 days from birth. This temporary treatment results in survival of all mice after discontinuation of the PT treatment.[36]

Primers

The primers used in this study are listed in Table S2.

Production, purification, and characterization of the rAAV vectors, and dosing

The AAV vectors used in this study are based on AAV type 2 backbone, and infectious vectors were prepared by the AAV Vector Unit at ICGEB Trieste (https://www.icgeb.org/avu-core-facility.html) in HEK293 cells by a cross-packing approach, whereby the vector was packaged into AAV capsid 8, followed by a CsCl gradient purification, and the titers were determined by measuring the copy number of viral genomes in pooled, dialyzed gradient fractions, as previously described.[16] The sequence of the primers used for quantification are listed in Table S2. Mice were injected neonatally via the retro-orbital vein.

Long-range PCR

Genomic DNA was extracted from about 25 mg liver powder using Wizard SV Genomic DNA Purification System (Promega). gDNA diluted 1/10 was used to perform Long Range PCR with Expand Long Template PCR System (Roche) using primers listed in Table S2. PCR product was digested with NcoI-HF (New England Biolabs) or XhoI (New England Biolabs) and separated in agarose gel. Donor plasmid (201 pAAV-hUGT1a1 optimized EX4 NEWDONOR) undigested or digested with the selected restriction enzyme was used as control.

RNA, RT-PCR, and real-time PCR

Extraction from tissues was performed using about 25 mg liver and brain powder or directly one-half organ for the heart. Samples were homogenized using 500 μL NucleoZOL (Macherey-Nagel) and RNA prepared according to manufacture instructions.

The RNA concentration was determined using NanoDrop 1000 spectrophotometer (Thermo Fisher Scientific). Samples in which *Sa*Cas9 expression was evaluated were treated with DNase I (Roche) according to manufacturer instructions. RNA concentration was measured again with NanoDrop before retro-transcription step.

RNA extracted from mouse tissues was retro-transcribed to obtain a template cDNA for quantitative teal-time PCR analysis. Reaction was performed using Moloney Murine Leukemia Virus Reverse Transcriptase (Thermo Fisher scientific) and Oligo (dT) primers.

qPCR was performed using the iQ SYBER Green Supermix (Bio-Rad) and a C1000 Thermal Cycler CFX96 Real Time System (Bio-Rad). Data were analyzed using the ΔΔCt method.

Expression of the gene of interest was normalized to Albumin to estimate the relative expression of *Sa*Cas9 in liver, to *GAPDH* for quantification of Cas9 RT-PCR in liver heart and brain, to Tubulin to compare liver and heart in qPCR.

Sequencing of cDNA

Liver RNA isolation of 25 mg powder was performed with NucleoZOL solution (Macherey-Nagel) as described in the RNA preparation section. One microgram of RNA was used to synthesize the cDNA with iScript Reverse Transcription Supermix (BioRad) according to manufacturer instructions. One microliter of cDNA undiluted was used to perform PCR, with Go Taq G2 Flexi Promega DNA Polymerase (Promega) and the primers listed in Table S1. PCR product was purified by agarose gel and cloned into pGEM T-Easy Vector System (Promega). Positive clones (white colonies) were Sanger sequenced and aligned with the mouse WT cDNA and the mutated sequence to verify the correction of the allele.

T7E1 assay

The T7E1 assay was performed following the manufacturer's instructions (New England Biolabs). Amplicons obtained from allele specific PCR were purified with Illustra MicroSpin S-400 HR columns (GE Healthcare). The PCR product was annealed in a SimpliAmp Thermal Cycler (Thermo Fisher scientific) according to manufacturer's instructions. Amplicons were treated with the T7E1 enzyme. Digested and undigested mixes were visualized on an agarose gel.

Total proteins extracts and western blot

Total proteins extraction was performed using 1× RIPA buffer (Cell Signaling) and protease inhibitor cocktail (Roche) was added immediately before use. Protein concentration was determined by Bradford protein assay (BioRad). For the western blot analysis in Figure 2C 40 μg total liver extract were used, while in Figure 4D 100 μg total extract were used. We casted 10% SDS homemade gels as previously described.[35] After electrophoretic separation, protein samples were transferred onto a polyvinylidene fluoride (PVDF) membrane (Millipore) using semi-dry Lightning Blot (PerkinElmer). Western blot in Figure 2C was performed by blocking with 5% milk PBS-Tween 0.1% for 2 h at room temperature and then incubated overnight with rabbit polyclonal IgG anti-UGT1A1 (Millipore) diluted 1:5,000 in 5% milk PBS-Tween 0.1% or with rabbit polyclonal IgG anti-Actin (Sigma-Aldrich) diluted 1:3,000 in 5% milk PBS-Tween 0.1%. The next day, membranes were washed and incubated with goat anti-rabbit horseradish peroxidase (HRP)-conjugated IgG (Dako) diluted 1:2,000 in PBS-Tween 0.1% for 1 h at room temperature. Detection of immuno-reactive bands was performed adopting enhanced chemiluminescent method (Clarity Western ECL Blotting Substrate, BioRad) and visualized with ChemiDoc imaging system (BioRad). Western blot in Figure 4D was performed by blocking the PVDF membrane (Immobilon-P, Millipore) with Immobilon Block-CH (Millipore) for 4 h at room temperature and then incubated overnight with affinity-purified rabbit IgG anti-UGT1A1 antibody (A01865-1, 1:2000, Boster Biological Technology Co) in 5% milk PBS-Tween 0.1%. Membrane was washed and incubated with goat anti-rabbit HRP-conjugated IgG (Dako) diluted 1:3,000 in PBS-Tween 0.1% for 1 h at room temperature. Detection of immuno-reactive bands was performed with ECL (Pierce ECL Western, Thermo Fisher Scientific) and Amersham Hyperfilm ECL system (GE Healthcare). Actin was used as a loading control.

Liver histology

Liver biopsies from Ugt1a$^{+/+}$, Ugt1a$^{-/-}$, and Ugt1a$^{-/-}$ treated animals were extracted and fixed with 10% formalin overnight at 4°C and then preserved in 20% sucrose 0.02% sodium azide at 4°C.

Paraffin-embedded sections (4 μm) were stained with hematoxylin and eosin or Masson's Trichrome staining as previously described.[47]

For immunofluorescence analysis, specimens were frozen in optimal cutting temperature media (BioOptica, Milano, Italy) and 4-μm slices were obtained in a cryostat. For Ugt1a, immunofluorescence liver specimens were incubated in 10 mM sodium citrate pH6 prior to blocking solution. Next, specimens were blocked in 10% normal goat serum (Dako) and then incubated with the anti-Ugt1a primary antibody (1:100; SAB2701158, Sigma) for 2 h at room temperature. Specimens were incubated 1 h with anti-rabbit secondary antibody Alexa Fluor 6478, Invitrogen). Nuclei were visualized by adding Hoechst (10 μg/mL) and mounted with Mowiol 4-88 (Sigma). Images were acquired with NIKON Fluorescence Upright Microscope Ni-U (100-240V) with HAMAMATSU Digital Camera (ORCA-Fash 4.0 V3 digital CMOS, Hamahatsu Photonics). Digital images were collected with NIS-Elements (Nikon) software.

NGS of ON target and OFF targets

Off-target loci were predicted using four online free software packages: the CasOffinder software (http://www.rgenome.net/cas-offinder/), CHOPCHOP (https://chopchop.cbu.uib.no), CCTOP (https://cctop.cos.uni-heidelberg.de), and CRISPOR (http://crispor.tefor.net).

All four software predicted the same off-targets loci for NcoI-gRNA with a cut-off mismatching of three mismatches. Since the present work was performed in FVN/NJ mouse strain we further proceeded

with CRISPOR program, since the genomic WT sequence of the stain was included in the genome options. The program predicted one on-target locus (*Ugt1a*) and four off-target loci; three of the four were in the introns of *Rtkn2*, *Wwox*, and *Nmnat3*, respectively, while one of the four was located in an intragenic region of chromosome 7 (*chr7-Olrf545*).

DNA from Ugt1a$^{-/-}$-untreated (n = 2) and -treated (n = 4) animals were extracted and the predicted on- and off-target regions were PCR amplified using Expand Long Template PCR system (Roche), which relies on the activity of a thermostable Taq DNA polymerase and Tgo DNA polymerase with 3′-5′ exonuclase activity (proof-reading). The primers used for PCR are listed in Table S1 and contain the complementary regions and a 5′ tail (33-mer) for the NGS sequencing procedures. For the on-target locus a first long PCR (4,290 bp), spanning the region external to the donor vector, was performed to avoid the amplification of the AAV episomes. The PCR was gel purified, and a second short PCR (409 bp) was performed using specific primers with tails. PCR products for off-target loci were in the range of 460–540 bp (461 bp, *Rtkn2*; 480 bp, *Wwox*; 486 bp, *Nmnat3*; and 542 bp, *chr7-Olrf545).* For each mouse, a mix of the six PCR was prepared to obtain a final concentration of 10 ng/μL for each targets and sent to BMR Genomic (BMR Genomic) for Illumina sequencing.

Raw sequencing data in FASTQ format were subjected to quality control and filtering using FastQC[48] and Trim Galore.[49] The resulting high-quality reads were subsequently aligned to Ensembl Mouse Reference genome (Mus_musculus_fvbnj.FVB_NJ_v1). The Burrows-Wheeler aligner[50] software was utilized for read alignment using standard parameters and the resulting alignments were sorted and indexed using Samtools.[51] Realignment and recalibration model was constructed using the suggested parameters as implemented in LoFreq (version 2).[52] Variants and INDELs were identified using LoFreq using standard parameters. Quality control measures and modified filters were applied to remove noise and minimize potential false positives, resulting in a high-confidence variants. A post-processing pipeline in the Bioconductor/R environment[53] was applied to further refine the variant calls. In particular, we selected the variants that have met the following criteria. (1) The variant had to pass the quality filter (QUAL) (2) to reduce noise variant calls, the variant had to be called with alternate frequency (AF) at least at 1% in one sample and the difference between treated and non-treated be at least 1%. (3) The read depth had to be greater than 100. (4) Finally, manual inspection was performed using IGV[54] to remove variants due the artifacts. To visualize the variants, we utilized CrispRVariants[55] R package starting from the BAM file obtained by the LoFreq pipeline.

Statistics

The Prism package (GraphPad Software) was used to analyze the data. The normal distribution of the data was confirmed with the Shapiro-Wilk test of normality. Depending on the experimental design, Student's t test, or one-way or two-way ANOVA, with Bonferroni's *post hoc* comparison tests, was used, as indicated in the legends to the figures and text. Results are expressed as mean ± SD. Values of $p < 0.05$ were considered statistically significant.

DATA AND CODE AVAILABILITY

The materials presented here are available for distribution after the execution of an MTA with the ICGEB.

SUPPLEMENTAL INFORMATION

Supplemental information can be found online at https://doi.org/10.1016/j.omtm.2023.101161.

ACKNOWLEDGMENTS

The work was supported by ICGEB intramural funds. We would like to thank the staff of the ICGEB adeno-associated vector unit (AVU) and the Bioexperimentation facilities for technical support. We thank Marco Baralle for proofreading this manuscript.

AUTHOR CONTRIBUTIONS

G.B., L.B., and A.F.M. designed the experiments; G.B., A.I., F.P., F.F., C.G., C.D.M., V.R., A.D.C., O.J.O., L.Z., L.B., and A.F.M. conducted the experiments, analysis, and interpretation of the data; G.B. and A.F.M. wrote the manuscript; G.B., A.I., F.P., F.F., C.G., C.D.M., V.R., A.D.C., O.J.O., L.Z., L.B., and A.F.M. performed a critical appraisal, and manuscript reviewing and editing.

DECLARATION OF INTERESTS

G.B. and A.F.M. are inventors of patents describing liver gene transfer approaches for metabolic diseases and/or treatment of hyperbilirubinemia. The remaining authors declare no competing interests.

REFERENCES

1. Bortolussi, G., and Muro, A.F. (2018). Advances in understanding disease mechanisms and potential treatments for Crigler–Najjar syndrome. Expert Opinion on Orphan Drugs *6*, 425–439.
2. Bosma, P.J., Seppen, J., Goldhoorn, B., Bakker, C., Oude Elferink, R.P., Chowdhury, J.R., Chowdhury, N.R., and Jansen, P.L. (1994). Bilirubin UDP-glucuronosyltransferase 1 is the only relevant bilirubin glucuronidating isoform in man. J. Biol. Chem. *269*, 17960–17964.
3. Crigler, J.F., Jr., and Najjar, V.A. (1952). Congenital familial nonhemolytic jaundice with kernicterus. Pediatrics *10*, 169–180.
4. van der Veere, C.N., Sinaasappel, M., McDonagh, A.F., Rosenthal, P., Labrune, P., Odievre, M., Fevery, J., Otte, J.B., McClean, P., Burk, G., et al. (1996). Current therapy for Crigler-Najjar syndrome type 1: report of a world registry. Hepatology *24*, 311–315.
5. Watchko, J.F., and Tiribelli, C. (2013). Bilirubin-induced neurologic damage–mechanisms and management approaches. N. Engl. J. Med. *369*, 2021–2030.
6. Maisels, M.J., and McDonagh, A.F. (2008). Phototherapy for neonatal jaundice. N. Engl. J. Med. *358*, 920–928.
7. Fagiuoli, S., Daina, E., D'Antiga, L., Colledan, M., and Remuzzi, G. (2013). Monogenic diseases that can be cured by liver transplantation. Journal of Hepatology *59*, 595–612.
8. Adam, R., Karam, V., Delvart, V., O'Grady, J., Mirza, D., Klempnauer, J., Castaing, D., Neuhaus, P., Jamieson, N., Salizzoni, M., et al. (2012). Evolution of indications and results of liver transplantation in Europe. A report from the European Liver Transplant Registry (ELTR). Journal of Hepatology *57*, 675–688.

9. George, L.A., Ragni, M.V., Rasko, J.E.J., Raffini, L.J., Samelson-Jones, B.J., Ozelo, M., Hazbon, M., Runowski, A.R., Wellman, J.A., Wachtel, K., et al. (2020). Long-Term Follow-Up of the First in Human Intravascular Delivery of AAV for Gene Transfer: AAV2-hFIX16 for Severe Hemophilia B. Mol. Ther. *28*, 2073–2082.
10. George, L.A., Sullivan, S.K., Giermasz, A., Rasko, J.E.J., Samelson-Jones, B.J., Ducore, J., Cuker, A., Sullivan, L.M., Majumdar, S., Teitel, J., et al. (2017). Hemophilia B Gene Therapy with a High-Specific-Activity Factor IX Variant. N. Engl. J. Med. *377*, 2215–2227.
11. Nathwani, A.C., Reiss, U.M., Tuddenham, E.G., Rosales, C., Chowdary, P., McIntosh, J., Della Peruta, M., Lheriteau, E., Patel, N., Raj, D., et al. (2014). Long-term safety and efficacy of factor IX gene therapy in hemophilia B. N. Engl. J. Med. *371*, 1994–2004.
12. Nathwani, A.C., Rosales, C., McIntosh, J., Rastegarlari, G., Nathwani, D., Raj, D., Nawathe, S., Waddington, S.N., Bronson, R., Jackson, S., et al. (2011). Long-term safety and efficacy following systemic administration of a self-complementary AAV vector encoding human FIX pseudotyped with serotype 5 and 8 capsid proteins. Mol. Ther. : the journal of the American Society of Gene Therapy *19*, 876–885.
13. Rangarajan, S., Walsh, L., Lester, W., Perry, D., Madan, B., Laffan, M., Yu, H., Vettermann, C., Pierce, G.F., Wong, W.Y., et al. (2017). AAV5-Factor VIII Gene Transfer in Severe Hemophilia A. N. Engl. J. Med. *377*, 2519–2530.
14. Donsante, A., Miller, D.G., Li, Y., Vogler, C., Brunt, E.M., Russell, D.W., and Sands, M.S. (2007). AAV vector integration sites in mouse hepatocellular carcinoma. Science *317*, 477.
15. Donsante, A., Vogler, C., Muzyczka, N., Crawford, J.M., Barker, J., Flotte, T., Campbell-Thompson, M., Daly, T., and Sands, M.S. (2001). Observed incidence of tumorigenesis in long-term rodent studies of rAAV vectors. Gene Ther. *8*, 1343–1346.
16. Bortolussi, G., Zentillin, L., Vanikova, J., Bockor, L., Bellarosa, C., Mancarella, A., Vianello, E., Tiribelli, C., Giacca, M., Vitek, L., et al. (2014). Life-long correction of hyperbilirubinemia with a neonatal liver-specific AAV-mediated gene transfer in a lethal mouse model of Crigler-Najjar Syndrome. Hum. Gene Ther. *25*, 844–855.
17. Cunningham, S.C., Dane, A.P., Spinoulas, A., Logan, G.J., and Alexander, I.E. (2008). Gene delivery to the juvenile mouse liver using AAV2/8 vectors. Mol. Ther. : the journal of the American Society of Gene Therapy *16*, 1081–1088.
18. Wang, L., Wang, H., Bell, P., McMenamin, D., and Wilson, J.M. (2012). Hepatic gene transfer in neonatal mice by adeno-associated virus serotype 8 vector. Hum. Gene Ther. *23*, 533–539.
19. Gillmore, J.D., Gane, E., Taubel, J., Kao, J., Fontana, M., Maitland, M.L., Seitzer, J., O'Connell, D., Walsh, K.R., Wood, K., et al. (2021). CRISPR-Cas9 In Vivo Gene Editing for Transthyretin Amyloidosis. N. Engl. J. Med. *385*, 493–502.
20. Frangoul, H., Altshuler, D., Cappellini, M.D., Chen, Y.-S., Domm, J., Eustace, B.K., Foell, J., de la Fuente, J., Grupp, S., Handgretinger, R., et al. (2021). CRISPR-Cas9 Gene Editing for Sickle Cell Disease and β-Thalassemia. N. Engl. J. Med. *384*, 252–260.
21. Junge, N., Yuan, Q., Vu, T.H., Krooss, S., Bednarski, C., Balakrishnan, A., Cathomen, T., Manns, M.P., Baumann, U., Sharma, A.D., et al. (2018). Homologous recombination mediates stable Fah gene integration and phenotypic correction in tyrosinaemia mouse-model. World J. Hepatol. *10*, 277–286.
22. Yin, H., Xue, W., Chen, S., Bogorad, R.L., Benedetti, E., Grompe, M., Koteliansky, V., Sharp, P.A., Jacks, T., and Anderson, D.G. (2014). Genome editing with Cas9 in adult mice corrects a disease mutation and phenotype. Nat. Biotechnol. *32*, 551–553.
23. Chandler, R.J., Venturoni, L.E., Liao, J., Hubbard, B.T., Schneller, J.L., Hoffmann, V., Gordo, S., Zang, S., Ko, C.W., Chau, N., et al. (2021). Promoterless, Nuclease-Free Genome Editing Confers a Growth Advantage for Corrected Hepatocytes in Mice With Methylmalonic Acidemia. Hepatology *73*, 2223–2237.
24. Venturoni, L.E., Chandler, R.J., Liao, J., Hoffmann, V., Ramesh, N., Gordo, S., Chau, N., and Venditti, C.P. (2022). Growth advantage of corrected hepatocytes in a juvenile model of methylmalonic acidemia following liver directed adeno-associated viral mediated nuclease-free genome editing. Mol. Genet. Metabol. *137*, 1–8.
25. Mannucci, P.M., and Tuddenham, E.G.D. (2001). The Hemophilias — From Royal Genes to Gene Therapy. N. Engl. J. Med. *344*, 1773–1779.
26. Anguela, X.M., Sharma, R., Doyon, Y., Miller, J.C., Li, H., Haurigot, V., Rohde, M.E., Wong, S.Y., Davidson, R.J., Zhou, S., et al. (2013). Robust ZFN-mediated genome editing in adult hemophilic mice. Blood *122*, 3283–3287.
27. Barzel, A., Paulk, N.K., Shi, Y., Huang, Y., Chu, K., Zhang, F., Valdmanis, P.N., Spector, L.P., Porteus, M.H., Gaensler, K.M., et al. (2015). Promoterless gene targeting without nucleases ameliorates haemophilia B in mice. Nature *517*, 360–364.
28. Li, H., Haurigot, V., Doyon, Y., Li, T., Wong, S.Y., Bhagwat, A.S., Malani, N., Anguela, X.M., Sharma, R., Ivanciu, L., et al. (2011). In vivo genome editing restores haemostasis in a mouse model of haemophilia. Nature *475*, 217–221.
29. Lisjak, M., De Caneva, A., Marais, T., Barbon, E., Biferi, M.G., Porro, F., Barzel, A., Zentilin, L., Kay, M.A., Mingozzi, F., et al. (2022). Promoterless Gene Targeting Approach Combined to CRISPR/Cas9 Efficiently Corrects Hemophilia B Phenotype in Neonatal Mice. Frontiers in Genome Editing *4*.
30. Guan, Y., Ma, Y., Li, Q., Sun, Z., Ma, L., Wu, L., Wang, L., Zeng, L., Shao, Y., Chen, Y., et al. (2016). CRISPR/Cas9-mediated somatic correction of a novel coagulator factor IX gene mutation ameliorates hemophilia in mouse. EMBO Mol. Med. *8*, 477–488.
31. Wang, Q., Zhong, X., Li, Q., Su, J., Liu, Y., Mo, L., Deng, H., and Yang, Y. (2020). CRISPR-Cas9-Mediated In Vivo Gene Integration at the Albumin Locus Recovers Hemostasis in Neonatal and Adult Hemophilia B Mice. Molecular Therapy - Methods & Clinical Development *18*, 520–531.
32. Sharma, R., Anguela, X.M., Doyon, Y., Wechsler, T., DeKelver, R.C., Sproul, S., Paschon, D.E., Miller, J.C., Davidson, R.J., Shivak, D., et al. (2015). In vivo genome editing of the albumin locus as a platform for protein replacement therapy. Blood *126*, 1777–1784.
33. De Caneva, A., Porro, F., Bortolussi, G., Sola, R., Lisjak, M., Barzel, A., Giacca, M., Kay, M.A., Vlahoviček, K., Zentilin, L., et al. (2019). Coupling AAV-mediated promoterless gene targeting to SaCas9 nuclease to efficiently correct liver metabolic diseases. JCI Insight *4*.
34. Porro, F., Bortolussi, G., Barzel, A., De Caneva, A., Iaconcig, A., Vodret, S., Zentilin, L., Kay, M.A., and Muro, A.F. (2017). Promoterless gene targeting without nucleases rescues lethality of a Crigler-Najjar syndrome mouse model. EMBO Mol. Med. *9*, 1346–1355.
35. Bortolussi, G., Zentilin, L., Baj, G., Giraudi, P., Bellarosa, C., Giacca, M., Tiribelli, C., and Muro, A.F. (2012). Rescue of bilirubin-induced neonatal lethality in a mouse model of Crigler-Najjar syndrome type I by AAV9-mediated gene transfer. Faseb. J. *26*, 1052–1063.
36. Bortolussi, G., Baj, G., Vodret, S., Viviani, G., Bittolo, T., and Muro, A.F. (2014). Age-dependent pattern of cerebellar susceptibility to bilirubin neurotoxicity in vivo in mice. Disease models & mechanisms *7*, 1057–1068.
37. Porro, F., Bockor, L., De Caneva, A., Bortolussi, G., and Muro, A.F. (2014). Generation of Ugt1-deficient murine liver cell lines using TALEN technology. PLoS One *9*, e104816.
38. Fox, I.J., Chowdhury, J.R., Kaufman, S.S., Goertzen, T.C., Chowdhury, N.R., Warkentin, P.I., Dorko, K., Sauter, B.V., and Strom, S.C. (1998). Treatment of the Crigler-Najjar syndrome type I with hepatocyte transplantation. N. Engl. J. Med. *338*, 1422–1426.
39. Tsuji, S., Stephens, C.J., Bortolussi, G., Zhang, F., Baj, G., Jang, H., de Alencastro, G., Muro, A.F., Pekrun, K., and Kay, M.A. (2022). Fludarabine increases nuclease-free AAV- and CRISPR/Cas9-mediated homologous recombination in mice. Nat. Biotechnol. *40*, 1285–1294.
40. Song, J., Yang, D., Xu, J., Zhu, T., Chen, Y.E., and Zhang, J. (2016). RS-1 enhances CRISPR/Cas9- and TALEN-mediated knock-in efficiency. Nat. Commun. *7*, 10548.
41. Fong, S., Handyside, B., Sihn, C.-R., Liu, S., Zhang, L., Xie, L., Murphy, R., Galicia, N., Yates, B., Minto, W.C., et al. (2020). Induction of ER Stress by an AAV5 BDD FVIII Construct Is Dependent on the Strength of the Hepatic-Specific Promoter. Molecular Therapy - Methods & Clinical Development *18*, 620–630.
42. Borel, F., Tang, Q., Gernoux, G., Greer, C., Wang, Z., Barzel, A., Kay, M.A., Shultz, L.D., Greiner, D.L., Flotte, T.R., et al. (2017). Survival Advantage of Both Human Hepatocyte Xenografts and Genome-Edited Hepatocytes for Treatment of alpha-1 Antitrypsin Deficiency. Mol. Ther. : the journal of the American Society of Gene Therapy *25*, 2477–2489.
43. Arnaoutova, I., Zhang, L., Chen, H.-D., Mansfield, B.C., and Chou, J.Y. (2021). Correction of metabolic abnormalities in a mouse model of glycogen storage disease type Ia by CRISPR/Cas9-based gene editing. Mol. Ther. *29*, 1602–1610.
44. Yang, Y., Wang, L., Bell, P., McMenamin, D., He, Z., White, J., Yu, H., Xu, C., Morizono, H., Musunuru, K., et al. (2016). A dual AAV system enables the

Cas9-mediated correction of a metabolic liver disease in newborn mice. Nat. Biotechnol. *34*, 334–338.

45. Lee, C.M., Davis, T.H., and Bao, G. (2018). Examination of CRISPR/Cas9 design tools and the effect of target site accessibility on Cas9 activity. Exp. Physiol. *103*, 456–460.
46. Heyer, W.-D., Ehmsen, K.T., and Liu, J. (2010). Regulation of Homologous Recombination in Eukaryotes. Annu. Rev. Genet. *44*, 113–139.
47. Collaud, F., Bortolussi, G., Guianvarc'h, L., Aronson, S.J., Bordet, T., Veron, P., Charles, S., Vidal, P., Sola, M.S., Rundwasser, S., et al. (2019). Preclinical Development of an AAV8-hUGT1A1 Vector for the Treatment of Crigler-Najjar Syndrome. Molecular therapy Methods & clinical development *12*, 157–174.
48. Andrews, S. (2010). FastQC: A Quality Control Tool for High Throughput Sequence Data. http://www.bioinformatics.babraham.ac.uk/projects/fastqc/.
49. Martin, M. (2011). Cutadapt removes adapter sequences from high-throughput sequencing reads. EMBnetjournal *17*, 10.
50. Li, H., and Durbin, R. (2009). Fast and accurate short read alignment with Burrows–Wheeler transform. Bioinformatics *25*, 1754–1760.
51. Danecek, P., Bonfield, J.K., Liddle, J., Marshall, J., Ohan, V., Pollard, M.O., Whitwham, A., Keane, T., McCarthy, S.A., Davies, R.M., et al. (2021). Twelve years of SAMtools and BCFtools. GigaScience *10*.
52. Wilm, A., Aw, P.P.K., Bertrand, D., Yeo, G.H.T., Ong, S.H., Wong, C.H., Khor, C.C., Petric, R., Hibberd, M.L., and Nagarajan, N. (2012). LoFreq: a sequence-quality aware, ultra-sensitive variant caller for uncovering cell-population heterogeneity from high-throughput sequencing datasets. Nucleic Acids Res. *40*, 11189–11201.
53. Marini, F., Linke, J., and Binder, H. (2020). ideal: An R/bioconductor package for interactive differential expression analysis. Preprint at bioRxiv. https://doi.org/10.1101/2020.01.10.901652.
54. Robinson, J.T., Thorvaldsdóttir, H., Wenger, A.M., Zehir, A., and Mesirov, J.P. (2017). Variant Review with the Integrative Genomics Viewer. Cancer Res. *77*, e31–e34.
55. Lindsay, H., Burger, A., Biyong, B., Felker, A., Hess, C., Zaugg, J., Chiavacci, E., Anders, C., Jinek, M., Mosimann, C., et al. (2016). CrispRVariants charts the mutation spectrum of genome engineering experiments. Nat. Biotechnol. *34*, 701–702.